Lysosome-like compartments of *Trypanosoma cruzi* trypomastigotes may originate directly from epimastigote reservosomes

JULIANA C. VIDAL[1,2]*, CAROLINA DE L. ALCANTARA[1,2], WANDERLEY DE SOUZA[1,2] *and* NARCISA L. CUNHA-E-SILVA[1,2]

[1] *Instituto de Biofísica Carlos Chagas Filho, Universidade Federal do Rio de Janeiro, Rio de Janeiro, Brazil*
[2] *Instituto Nacional de Ciência e Tecnologia em Biologia Estrutural e Bioimagens, Rio de Janeiro, Brazil*

(*Received 16 September 2016; revised 21 November 2016; accepted 3 December 2016; first published online 12 January 2017*)

SUMMARY

Trypanosoma cruzi epimastigote reservosomes store nutrients taken up during the intense endocytic activity exhibited by this developmental form. Reservosomes were classified as pre-lysosomal compartments. In contrast, trypomastigote forms are not able to take up nutrients from the medium. Interestingly, trypomastigotes also have acidic organelles with the same proteases contained in epimastigote reservosomes. Nevertheless, the origin and function of these organelles have not been disclosed so far. Given the similarities between the compartments of epimastigotes and trypomastigotes, the present study aimed to investigate the origin of metacyclic trypomastigote protease-containing organelles by tracking fluorospheres or colloidal gold particles previously stored in epimastigotes' reservosomes throughout metacyclogenesis. Using three-dimensional reconstruction of serial electron microscopy images, it was possible to find trypomastigote compartments containing the tracer. Our observations demonstrate that the protease-containing compartments from metacyclic trypomastigotes may originate directly from the reservosomes of epimastigotes.

Key words: *Trypanosoma cruzi*, metacyclogenesis, trypomastigotes, lysosome-like organelles, reservosomes.

INTRODUCTION

Trypanosoma cruzi is the aetiological agent of Chagas disease. During the biological cycle of *T. cruzi*, three different forms are found. Epimastigotes are the main proliferative forms in the insect vector and undergo the metacyclogenesis process, changing to non-dividing, infective, metacyclic trypomastigote forms, which are released with the feces of the insect. In the vertebrate host, amastigotes and trypomastigotes are released from the infected host cells after a complex intracellular life cycle (De Souza, 2002). Epimastigotes have intense endocytic activity, taking up nutrients from the insect blood meal such as cholesterol and sources of amino acids and lipids (Soares and de Souza, 1991). Nutrients are ingested through specialized sites, the cytostome–cytopharynx and flagellar pocket, at the anterior region of the parasite body, and are delivered to reservosomes, which are typically located at the posterior end. Reservosomes are the last compartment of the endocytic pathway, provide storage for macromolecules and also concentrate cruzipain (Soares *et al*. 1992), the most abundant *T. cruzi* protease. These organelles are able to digest macromolecules, present an acidic pH, maintained by unusual P-type H^+ ATPases (Vieira *et al*. 2005), and contain internal laminar membranes and vesicles (Sant'Anna *et al*. 2008*b*). Although a complete proteomic analysis of purified reservosomes has already been performed (Sant'Anna *et al*. 2009), a molecular marker has not been determined thus far, as none of the highest hits of the proteomics, as p67 and TcHA3, a P-type H^+ ATPase isoform, was validated as bona fide molecular markers yet, being present exclusively in reservosomes. Meanwhile, the accumulation of cruzipain, that is also present at the plasma membrane and at Golgi complex, has been used as a tool to identify reservosomes. Despite the above described characteristics, reservosomes were not considered genuine lysosomes because they lack typical lysosomal markers, such as lysosome-associated membrane proteins (LAMPs), and had their internal pH evaluated as 6·0 by an immune electron microscopy technique (Soares *et al*. 1992). Thereby, reservosomes were classified as pre-lysosomal compartments (Soares *et al*. 1992).

A stereological study of reservosomes in the course of *in vitro* metacyclogenesis in chemically defined media revealed that their content was massively degraded, leading to the conclusion that the organelle 'disappears' during this process, probably due to the consumption of the proteins and lipids stored therein (Soares *et al*. 1989). The metacyclic trypomastigotes generated at the end of this process are unable to take up macromolecules from the medium (de Souza *et al*. 2009). Nevertheless, they contain organelles

* Corresponding author: Instituto de Biofísica Carlos Chagas Filho, Universidade Federal do Rio de Janeiro, Rio de Janeiro, Brazil and Instituto Nacional de Ciência e Tecnologia em Biologia Estrutural e Bioimagens, Rio de Janeiro, Brazil. E-mail: vidal.ju@gmail.com

Parasitology (2017), **144**, 841–850.
doi:10.1017/S0031182016002602

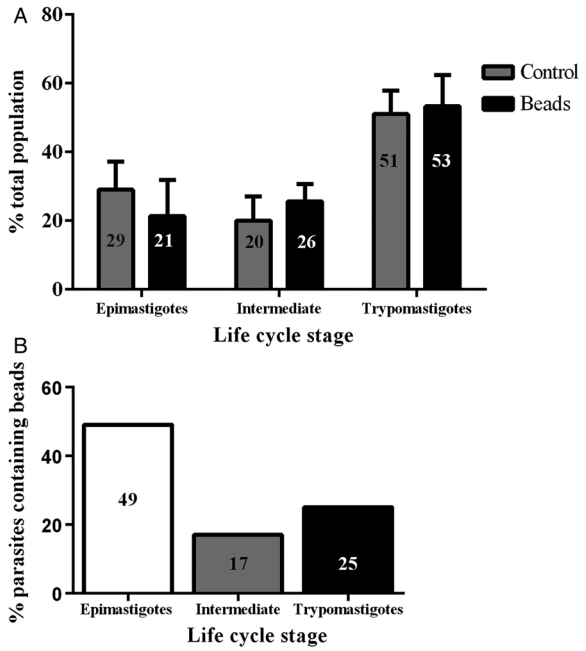

Fig. 1. Previous endocytosis did not affect metacyclogenesis. The two graphs contain complementary information. (A) Independent and simultaneous differentiation experiments were performed using epimastigotes preloaded or not (control, grey columns) with 40 nm fluorescent beads (black columns). Parasite forms were counted after 72 h of differentiation, irrespective of containing beads or not. The percentage of epimastigote differentiation into trypomastigotes was similar. The experiment was repeated three times ($N = 3$). Variance tested by two-way ANOVA and Bonferroni post-test obtained $P > 0{\cdot}05$. (B) Only parasites that still contained beads after 72 h were counted, and the percentage they represented within that parasite form was calculated. One fourth of the metacyclic trypomastigotes contained beads inside.

that share many features with reservosomes: they are slightly electron-dense, have internal vesicles and lipid inclusions, and contain cruzipain, chagasin, serine carboxypeptidase and P-type H^+ ATPase concentrated in an acidic environment, being classified as lysosome-related organelles (LROs) (Sant'Anna *et al*. 2008*a*). At this time there was no evidence of the origin of these trypomastigote acidic organelles.

Differentiation of epimastigotes into trypomastigotes is accompanied by extensive metabolic and morphological changes to enable parasite adaptation to environmental transitions. In the present study, we have accompanied the fate of reservosome content during metacyclogenesis and managed to demonstrate that the so-called LROs of metacyclic trypomastigotes may arise directly from reservosomes.

MATERIAL AND METHODS

Parasites

Trypanosoma cruzi epimastigotes from the Dm28c clone were cultivated in liver infusion tryptose (LIT) (Camargo, 1964) supplemented with 10% (v/v) fetal calf serum (FCS) at 28 °C. Stationary-phase parasites from 6-day-old cultures were used in all experiments.

We have also used transfected Dm28c parasites with the green fluorescent protein (GFP) gene integrated in the chromosome carrying the ribosomal cistron. Only the proliferative forms (epimastigotes and amastigotes) of this mutant *T. cruzi* cell line, named pBEX/GFP, express large amounts of GFP. It is likely that during metacyclogenesis, the parasites lose their fluorescence as they evolve throughout differentiation, allowing for the identification of late intermediate cells by flow cytometry.

Endocytic tracers

Colloidal gold particles (Au, 8–10 nm) were prepared according to (Slot and Geuze, 1985). Bovine holotransferrin (Sigma, St. Louis, USA) was coupled to gold particles as described (Roth, 1983) and used as an endocytic tracer (Tf-Au). Alternatively, 40 nm red carboxylate-modified fluorospheres (580/605, Life Technologies, Carlsbad, USA) were used.

Endocytosis assays associated with metacyclogenesis: stationary phase

Epimastigotes were collected by centrifugation at 1500 ***g*** for 10 min, washed twice in phosphate-buffered saline [PBS; 10 mM sodium phosphate buffer pH 7·2 plus 0·9% (w/v) NaCl], and incubated in LIT containing Tf-Au or red fluorospheres for 30 min at 28 °C. Subsequently, the cells were washed twice in LIT and then incubated in LIT containing 10% FCS for 1 h in order to accumulate the tracer in reservosomes (Soares and de Souza, 1991). These parasites will be designated as preloaded epimastigotes. After 1 h, the preloaded epimastigotes were washed and metacyclogenesis was induced.

In vitro metacyclogenesis

Epimastigotes, preloaded or not with endocytic cargo, were induced to differentiate to metacyclic trypomastigotes (Contreras *et al*. 1985). Briefly, epimastigotes were collected by centrifugation at 3000 ***g*** for 30 min, washed once in triatomine artificial urine (TAU) medium (190 mM NaCl, 17 mM KCl, 2 mM $MgCl_2$, 2 mM $CaCl_2$, 8 mM sodium phosphate buffer, pH 6·0) and adjusted to 5×10^8 cells mL^{-1} in the same medium. After 2 h at 28 °C, the parasites were diluted 100-fold in TAU supplemented with 50 mM sodium glutamate, 10 mM L-proline, 2 mM sodium aspartate and 10 mM glucose (TAU3AAG) in cell culture flasks and maintained afterwards at 28 °C for 72 h. Cell fixation and staining were

https://doi.org/10.1017/S0031182016002602 Published online by Cambridge University Press

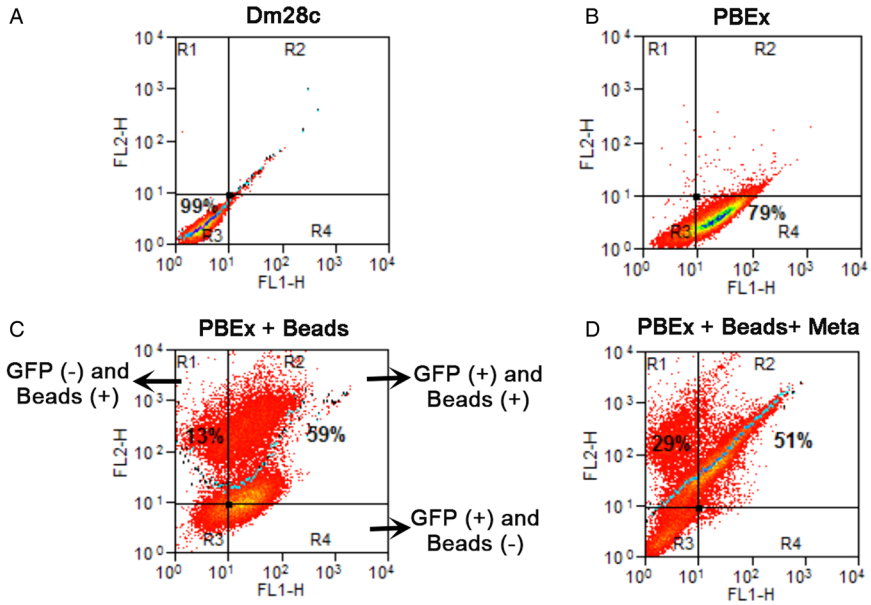

Fig. 2. Quantification of GFP and beads inside parasites by flow cytometry before and after metacyclogenesis. (A) The control population, Dm28c epimastigotes, was run in both channels and did not contain autofluorescence. (B) PBEx epimastigotes; 79% of the population was GFP-positive; (C) PBEx epimastigotes after bead endocytosis; 59% of the epimastigotes (GFP+) had taken up beads; 13% of the parasites had already lost their GFP signal. (D) Preloaded PBEx after metacyclogenesis; 51% of the population was GFP- and bead-positive, i.e. epimastigotes that did not differentiate. Approximately 29% of the intermediates and trypomastigotes (GFP-negative) were bead-positive.

performed using the Panoptic staining kit (Laborclin, Pinhais, Brazil), following the manufacturer's instructions. The panoptic staining was observed in a fluorescence microscope. Bright field images were used to determine the life cycle stage, and fluorescence images were used to detect the bead presence and cell localization.

Confocal laser scanning microscopy (CLSM)

Metacyclic trypomastigotes obtained from preloaded epimastigotes were fixed in 2·5% freshly prepared formaldehyde in PBS for 30 min, then washed and settled onto poly-L-lysine-coated coverslips. After rinsing in PBS and mounting with ProLong® DAPI Antifade (Vector Labs, Burlingame, CA, USA), the slides were examined in a LEICA TCS-SP5 CLSM.

Flow cytometry

After metacyclogenesis, the wild-type Dm28c and pBEx/GFP parasites were collected, washed in PBS and fixed in 1% formaldehyde in PBS. After 10 min, the cells were washed in PBS. The suspension containing a total population of 1×10^6 cells in 500 μL was read on a FACSCalibur [Becton Dickinson Biosciences (BDB), San Jose, CA, USA]; GFP fluorescence was analysed using the FL1-H detector (530/30 nm) and red fluorescence was detected using FL2-H (585/40 nm). A total of 30 000 events were acquired in the scatter regions previously shown to correspond to parasites.

Transmission electron microscopy (TEM)

Metacyclic parasites were fixed with 2·5% (v/v) glutaraldehyde in 0·1 M cacodylate buffer, pH 7·2, for 1 h at room temperature. The cells were washed twice in 0·1 M cacodylate buffer, pH 7·2, and post-fixed using an OTO protocol (for osmium–thiocarbohydrazide–osmium). Briefly, the cells were incubated in a post-fixative osmium solution [1% (v/v) osmium tetroxide, 0·8% (v/v) potassium ferrocyanide, 5 mM calcium chloride in 0·1 M cacodylate buffer, pH 7·2] for 40 min, washed twice in water and then incubated in a solution of 1% (w/v) thiocarbohydrazide (TCH – Sigma, St. Louis, USA) in water for 5 min. After three washes in water, the cells were incubated again in the post-fixative osmium solution for 3 min. Following post-fixation, the samples were washed in water, dehydrated in an acetone series and embedded in Epoxy resin. Ultrathin sections were stained with 5% (w/v) uranyl acetate and lead citrate (Reynolds, 1963) and observed on a Tecnai-G2 TEM operating at 200 kV.

Focused ion beam–scanning electron microscopy (FIB–SEM)

For observation by FIB–SEM, the metacyclic cells obtained from preloaded epimastigotes were processed for TEM as described above. The tips of resin blocks containing the sample were trimmed to a pyramidal shape and mounted on a support for FIB–SEM.

https://doi.org/10.1017/S0031182016002602 Published online by Cambridge University Press

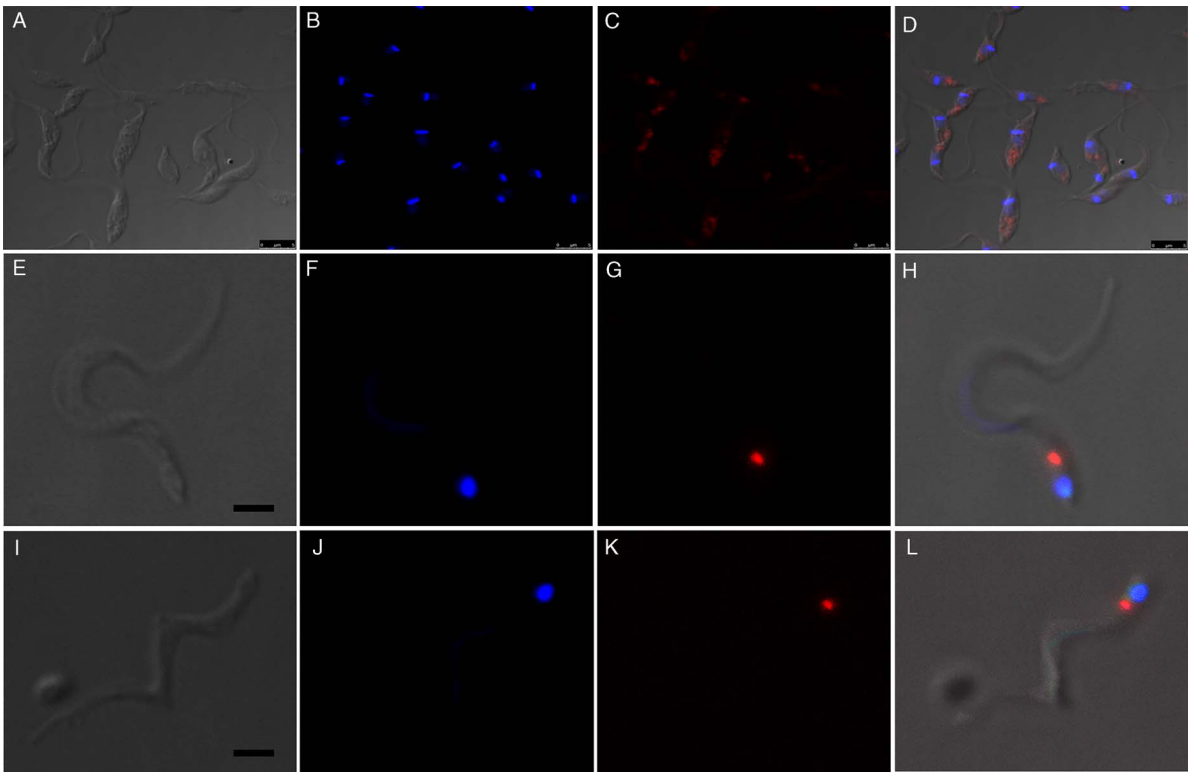

Fig. 3. Fluorescence images of preloaded parasites after 72 h of metacyclogenesis. (A–D) After the endocytosis assay, beads were localized in the reservosomes, typically at the posterior region of the epimastigotes. (E–L) Preloaded epimastigotes were allowed to undergo metacyclogenesis. After 72 h of differentiation, metacyclic trypomastigotes contained beads between the nucleus and kinetoplast. A, E, I, images of parasites obtained by differential interferential contrast. B, F, J, DAPI staining indicates the kinetoplast and nucleus positions. C, G, K red fluorescence from beads. D, H, L, merged images. Bars: 5 μm.

The images were recorded using a Helios 200 NanoLab dual-beam microscope (Eindhoven, NL, USA) equipped with a gallium ion source for focused-ion beam milling and a field-emission gun scanning electron microscope with an in-lens secondary electron detector for imaging. To create a slice-and-view image series, a step size of 25 nm was chosen for the removal of material from the specimen surface. After image capturing, the contrast of back-scattered electron images was inverted so that they resembled conventional TEM images. The sequential slices were automatically aligned using the XfAlign algorithm of IMOD, and a fine alignment was then performed using MIDAS. All three-dimensional (3D) models and measurements were performed with 3DMOD.

RESULTS

Preloading of reservosomes did not affect metacyclogenesis

Epimastigotes were incubated with 40 nm fluorescent beads or 10 nm Tf-Au in the LIT medium for 30 min at 28 °C. Subsequently, the tracers were washed out and the parasites incubated for additional 30 min in LIT at 28 °C to concentrate the tracers in reservosomes before proceeding with metacyclogenesis. The rate of endocytosis in the epimastigotes was quantified by counting on a fluorescence microscope. Approximately 60% of the epimastigotes had accumulated beads in their reservosomes (not shown). To evaluate whether the preloading of the reservosomes with beads interfered with metacyclogenesis, we handled two populations in parallel, one with epimastigotes that had taken up beads and another with epimastigotes that were manipulated in the same way but without the tracer (control). After 72 h of metacyclogenesis, we counted the proportion of the developmental stages and found that the rate of metacyclogenesis was not affected by the previous loading of reservosomes: the percentage of trypomastigotes derived from epimastigotes preloaded with beads was similar to the percentage of trypomastigotes derived from epimastigotes that did not endocytose the beads (Fig. 1A).

Endocytic tracers were maintained after metacyclogenesis

Analysing only the population that was preloaded, we counted the parasites that maintained the beads after the differentiation period: 17% of the

https://doi.org/10.1017/S0031182016002602 Published online by Cambridge University Press

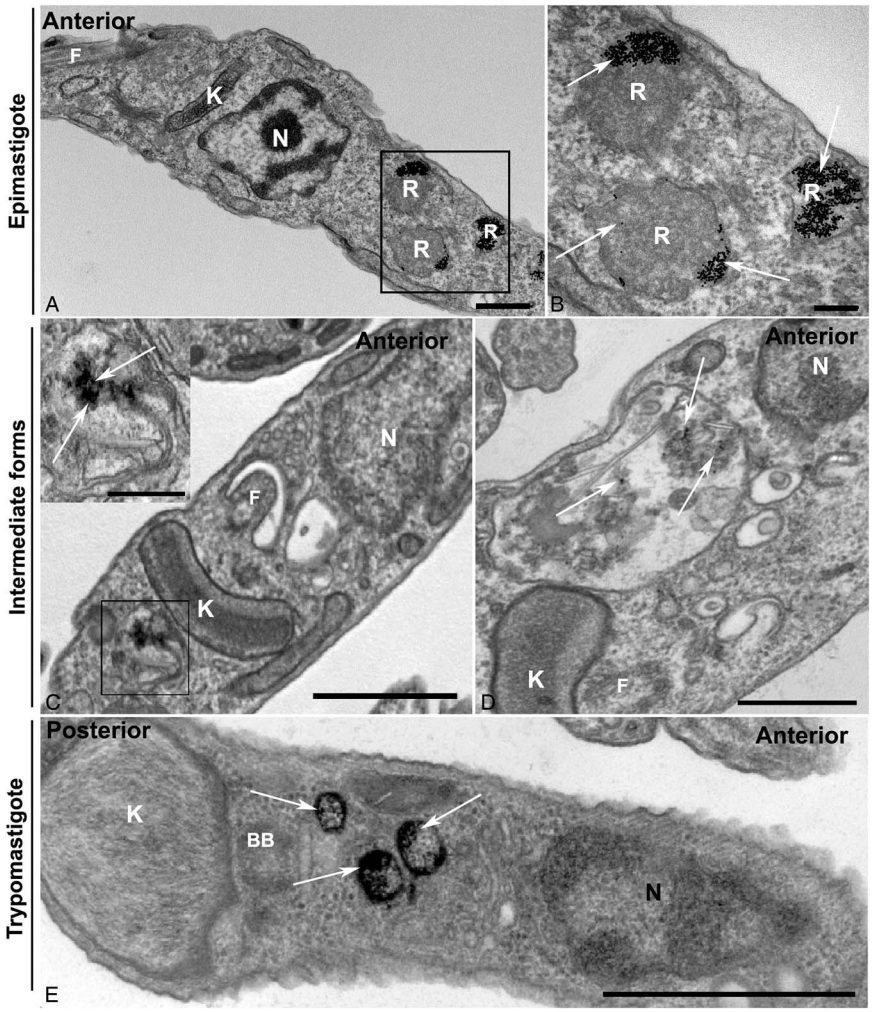

Fig. 4. Preloaded parasites with Tf-Au after 72 h of metacyclogenesis. (A and B) Control images. (A) Epimastigotes were incubated for 30 min with Tf-Au, washed to remove non-internalized tracer and maintained for 72 h in the LIT medium with 10% fetal calf serum. The tracer remained accumulated in reservosomes (R); (B) High magnification of square in A showing the maintenance of Tf-Au (arrows) in reservosomes after 72 h incubation in LIT B without tracer; (C and D) Parasites at the advanced intermediate stage of metacyclogenesis, before complete transformation into a trypomastigote form; (C) Intermediate form with a gold particle-containing compartment posterior to the disc-shaped kinetoplast (K) and to the nucleus. The inset shows a high magnification of the square in C with arrows pointing to the presence of gold particles; (D) Intermediate form with disc-shaped kinetoplast (K) posterior to nucleus (N). Observe the presence of gold particles (arrows) and lipid inclusions inside a big compartment similar to reservosomes, between kinetoplast and nucleus; (E) Trypomastigote form, after completely ultrastructural remodelling, showing rounded kinetoplast (K) posterior to the nucleus (N). Observe the presence of round organelles between nucleus (N) and kinetoplast (K) containing gold particles (arrows).

intermediate forms and 25% of the trypomastigotes still had beads inside rounded organelles (Fig. 1B). These results revealed not only that previous endocytosis did not interfere with metacyclogenesis, but also that the tracers could be maintained until the end of differentiation. We decided to use a stably transfected fluorescent clone of *T. cruzi* Dm28c, in which the GFP gene was integrated into the chromosome carrying the ribosomal cistron. These fluorescent parasites, named PBEx, produce detectable amounts of GFP only at replicative stages (Kessler *et al*. 2013). PBEx parasites were a valuable tool for flow cytometry, as they allowed for the distinction of epimastigotes, which expressed high amounts of GFP, from parasites undergoing metacyclogenesis, because the intermediates and trypomastigotes contained no GFP fluorescence. Thereby, the PBEx parasites were used to increase the number of parasites analysed (Fig. 2A–D). Seventy-nine per cent of the PBEx epimastigote population was GFP-positive (Fig. 2B). After red beads endocytosis, 59% of the PBEx epimastigotes were both GFP- and bead-positive, whereas 13% of the cells had already lost the GFP signal but contained red bead fluorescence (Fig. 2C). After 72 h in the differentiation medium, 51% of the preloaded PBEx population contained both signals (Fig. 2D), while 29% had lost the GFP signal and maintained

https://doi.org/10.1017/S0031182016002602 Published online by Cambridge University Press

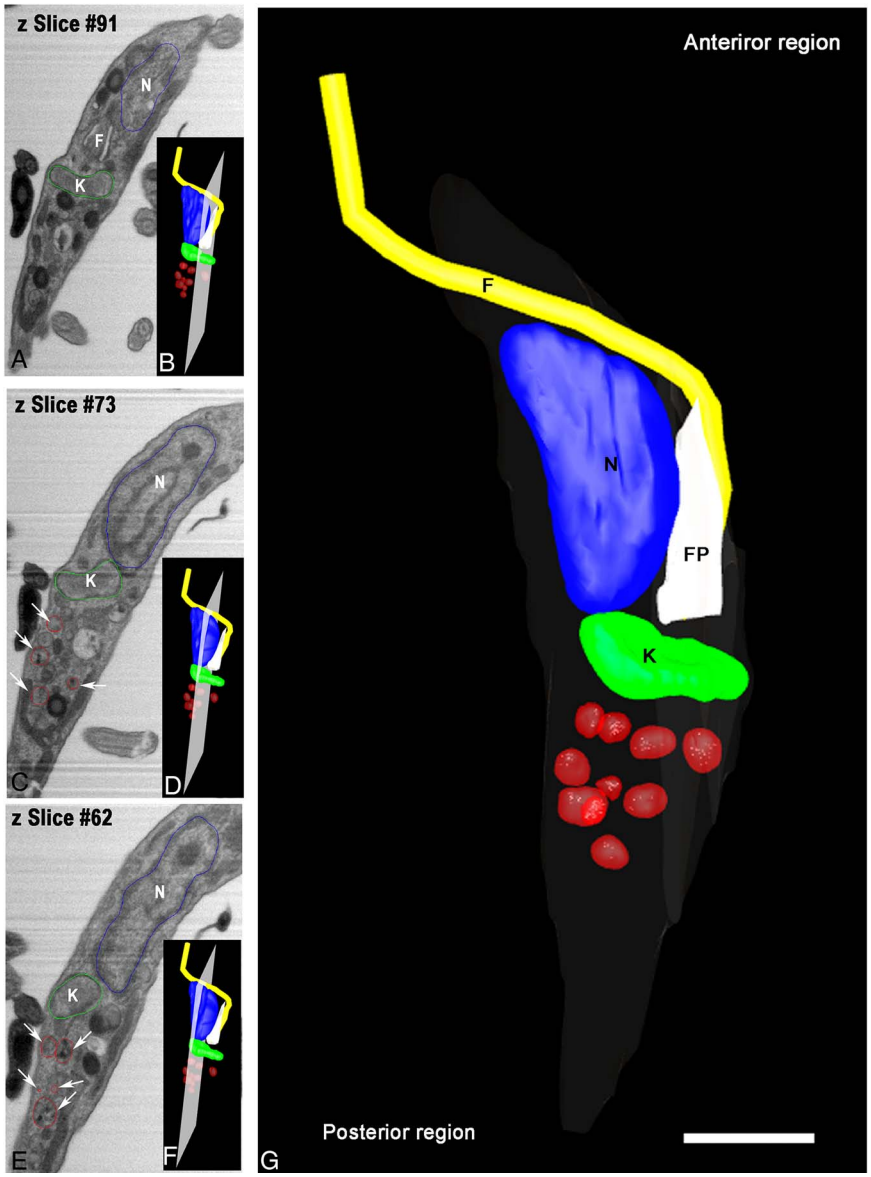

Fig. 5. Tridimensional reconstruction of a FIB–SEM series obtained from *T. cruzi* intermediate forms. (A and F) An intermediate showing a transversal view with kinetoplast (K) posterior to nucleus (N) and tracer-containing organelles (arrows) localized posterior to the kinetoplast. In B, D and F, the position and orientation of each Z-slice is indicated by a white rectangle. Scale bar: 100 nm. Membrane – grey, kinetoplast – green, nucleus – blue, flagellum – yellow, flagellar pocket – white, tracer-containing compartments – red.

the red bead fluorescence. These parasites were in fact intermediaries and trypomastigotes that still had beads inside the cell body.

Localization of beads after metacyclogenesis

Fluorescence images showed that in epimastigotes (before metacyclogenesis) the beads were inside compartments with size and localization typical of reservosomes (Fig. 3A–D). After 72 h of differentiation, the fluorescent tracers in the trypomastigotes were found in round organelles between the nucleus and the kinetoplast (Fig. 3E–L).

For a better observation of the fine structure of the parasites that had taken up Tf-Au before differentiation, the cells were analysed by transmission electron microscopy. Epimastigotes retained gold particles in reservosomes even after 72 h in LIT containing 10% FCS without the endocytic tracer (Fig. 4A and B). After 72 h of metacyclogenesis, we observed intermediate forms with organelles that were morphologically similar to reservosomes containing Tf-Au (Fig. 4C and D). Gold particles were also seen inside round-shaped organelles of advanced intermediate forms that had almost achieved the trypomastigote stage, as the parasite depicted in Fig. 4D. These organelles had electron-lucent inclusions, as observed in epimastigote reservosomes. In trypomastigotes (Fig. 4E), we found Tf-Au accumulated in round-shaped

https://doi.org/10.1017/S0031182016002602 Published online by Cambridge University Press

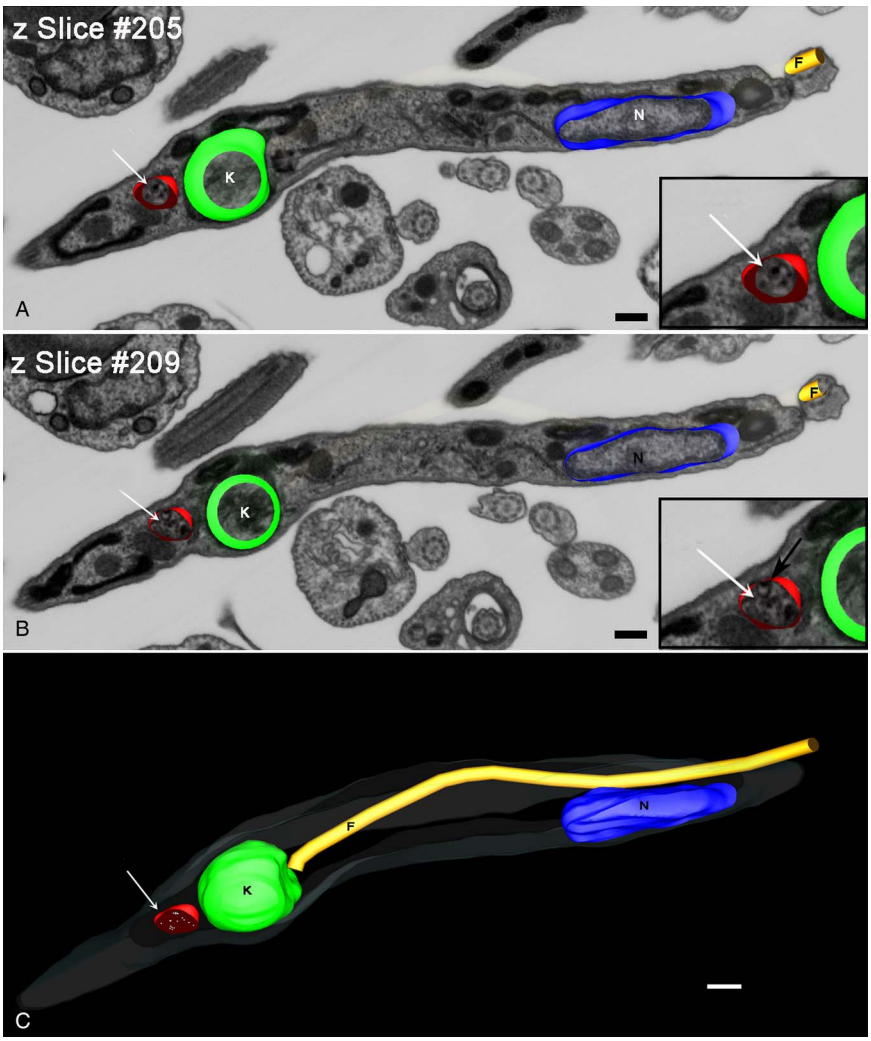

Fig. 6. *Z*-planes of FIB–SEM series of a metacyclic trypomastigote. (A and B) Planes 205 (A) and 209 (B) of a trypomastigote with tracer-containing compartment (arrow). This compartment contains Tf-Au (insets in A and B) that had been taken up by the epimastigotes before differentiation and also inner vesicles (inset in B-black arrow). (C) 3D-reconstruction clarified the position posterior to the kinetoplast and the round form of this trypomastigote tracer-containing compartment (arrow). Bars: 20 nm. Membrane – grey, kinetoplast – green, nucleus – blue, flagellum – yellow, tracer-containing compartments – red.

organelles localized between the nucleus and the typically spherical kinetoplast of this stage, corroborating the fluorescence microscopy analysis.

Aiming to examine more parasites, we obtained serial images using FIB–SEM, also referred to as ion abrasion SEM (Drobne *et al*. 2008), to generate a stack of 2D EM images. These images were computationally converted to a 3D ultrastructural volume of the sample. FIB–SEM represents a tool that allows for the reconstruction of whole cells from sections much thinner than could be obtained by serial sectioning with an ultramicrotome. For this purpose, we utilized resin-embedded parasites that were preloaded with Tf-Au and allowed to undergo metacyclogenesis for 72 h. In order to accompany the ultrastructural changes in reservosomes, we reconstructed an intermediate form in a longitudinal orientation (Fig. 5A–E). This intermediate already had the kinetoplast positioned posterior to the nucleus, although its form was not completely spherical. We observed numerous tracer-containing organelles localized posterior to the kinetoplast (Fig. 5B–D).

The reconstruction of a trypomastigote in a longitudinal orientation (Fig. 6) revealed a structure the size of tracer-containing organelle localized posterior to the kinetoplast. This organelle appeared smaller than reservosomes but with the spherical shape maintained, with many gold particles dispersed in the lumen (Fig. 6A and B insets). Note that it was possible to visualize the inner membranes in tracer-containing organelle (Fig. 6B inset – black arrow), which were similar to those described in reservosomes.

A trypomastigote, reconstructed from the same preparation, showed organelles filled with Tf-Au

https://doi.org/10.1017/S0031182016002602 Published online by Cambridge University Press

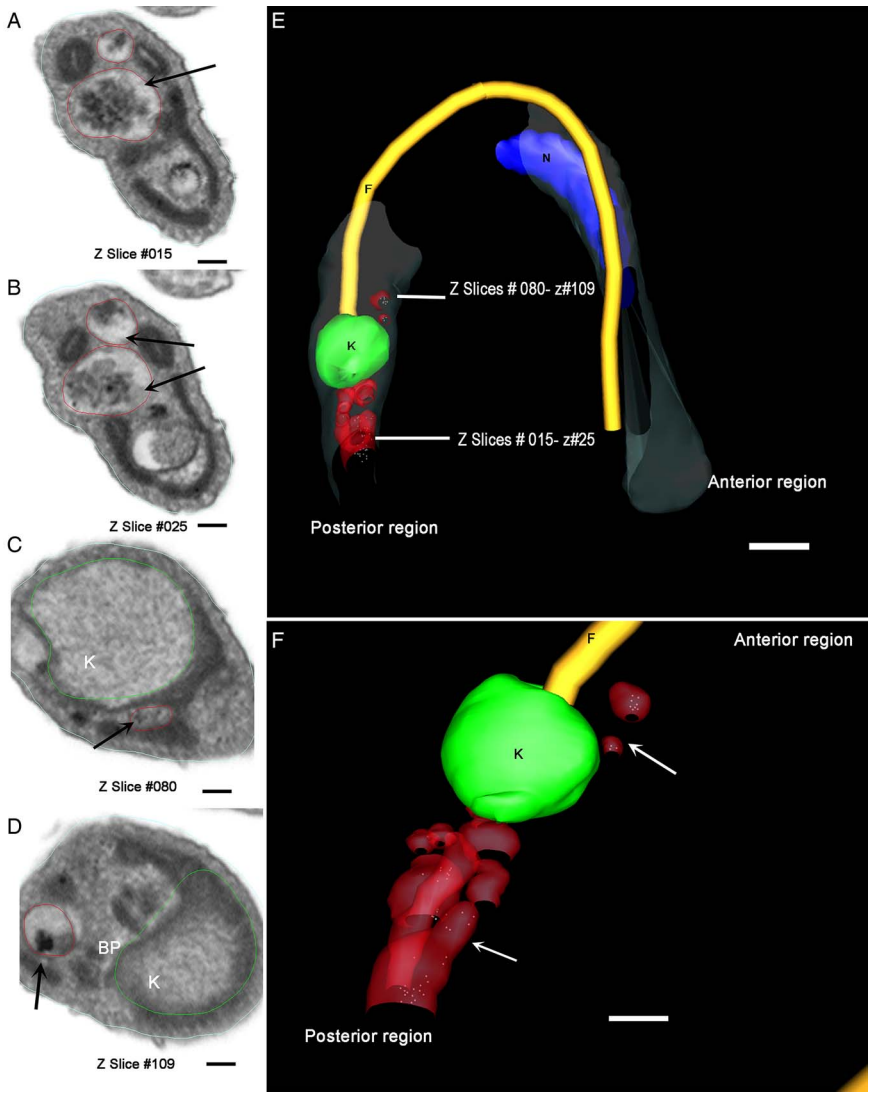

Fig. 7. Different *z*-planes of a FIB–SEM series of preloaded parasites after metacyclogenesis. (A–D) Transversal slice images of a metacyclic trypomastigote, showing different regions of the cell body with organelles filled with Tf-Au. (E) The 3D-reconstruction was obtained and rotated to allow the observation of the relative position of the Tf-Au filled organelles; (F) Magnification of the 3D-reconstruction: the tracer containing compartments (white arrows) were distributed not only between the nucleus and the kinetoplast, but also at the posterior end of the parasite. Bars: 50 nm. Membrane – grey, kinetoplast – green, nucleus – blue, flagellum – yellow, tracer-containing compartments – red.

not only between the nucleus and the kinetoplast, but also at the parasite's posterior end (Fig. 7A–F and Supplementary Material Movie 1). These compartments (tracer-containing organelles observed in Figs 5–7) have average diameter of 80·14 ± 6·9 nm ($n = 21$).

DISCUSSION

Data from the literature have shown that some factors hinder or prevent metacyclogenesis. Among them, treatment with cruzipain inhibitors (Franke de Cazzulo *et al*. 1994), inhibitors of proteasome activity (Cardoso *et al*. 2008) and the enrichment of metacyclogenesis medium (Figueiredo *et al*. 2000), interfering with the nutrient stress that triggers differentiation. Figueiredo *et al*. (2000) had shown that the addition of transferrin to TAU3AAG medium inhibited metacyclogenesis and promoted epimastigote proliferation, unlike the control experiment. In the present study, the quantification of the rates of metacyclogenesis of parasites that had been preloaded with transferrin-gold or fluorescent beads reached values similar to the control data. We were able to show that if the accumulation of a non-digestible tracer inside epimastigote reservosomes occurred before nutritional stress, metacyclogenesis was not impaired. Interestingly, if nutrients and tracers were offered after 48 h of differentiation, the intermediate forms, but not the trypomastigotes and the late intermediates that had already disassembled the cytostome, were capable of internalizing and accumulate tracers in reservosomes (Vidal *et al*. 2016).

https://doi.org/10.1017/S0031182016002602 Published online by Cambridge University Press

In tissue culture-derived trypomastigotes, protease-containing organelles were localized between the kinetoplast and the nucleus (Sant'Anna *et al*. 2008*a*). Now, working with intermediary forms of metacyclogenesis, we found the tracer-containing organelles in the extreme posterior region of the parasite body. At the end of metacyclogenesis, the tracer-containing compartments of trypomastigotes were also localized between nucleus and kinetoplast, besides the posterior extremity. This distribution may result from the course of the differentiation remodelling process. Although we could not document, the smaller size of tracer-containing compartments can suggest reservosome fragmentation during metacyclogenesis, as it average size (80 nm) contrast with the value of epimastigote reservosomes (420–500 nm) (Soares and De Souza, 1988; Soares *et al*. 1989). Trypomastigote organelles are morphologically distinct from reservosomes not only in size, but also in electron density. However, they contained the typical inner vesicles, the same ultrastructural pattern as reservosomes (Sant' Anna *et al*. 2008*b*). Moreover, metacyclic trypomastigotes' compartments contained Tf-Au, taken up by epimastigotes and retained in this organelle until the end of metacyclogenesis.

Nevertheless, the present data do not exclude other possible fates for the reservosome content and membrane, such as giving rise to exosomes. These extracellular vesicles have been detected in the differentiation medium (Trocoli Torrecilhas *et al*. 2009; Bayer-Santos *et al*. 2013; Garcia-Silva *et al*. 2014), most of them originating from plasma membrane and flagellar membrane shedding. One type of extracellular vesicle found inside the flagellar pocket seems to originate from an intracellular compartment, the multivesicular body that fuses with the flagellar pocket membrane (Bayer-Santos *et al*. 2013). In the course of the experiments that compose this work, we have never found preloaded reservosomes or multivesicular bodies, either from epimastigotes or from intermediate forms, fusing with or in the vicinities of the flagellar pocket.

Stereological studies had shown that reservosomes occupy approximately 5·6% of the total cell volume of epimastigotes but gradually disappear during differentiation to trypomastigote forms (Soares *et al*. 1989). It has been suggested that the nutrients accumulated in reservosomes could be used as the main energy source for this activity. The present data raise the question of whether reservosomes actually disappear in metacyclogenesis or may be remodelled by changing size, shape and distribution, and simply lose the ability to receive endocytic material, originating the so-called lysosome-related organelles – LROs – of trypomastigotes (Sant'Anna *et al*. 2008*a*).

Different from lysosomes, whose main function is to hydrolyse nutrients of extracellular origin, LROs have additional functions or a peculiar function correlated with the cell type. LROs are often referred as secretory lysosomes because they are capable of secretion their contents into the extracellular milieu. Thereby, the term LRO has been reserved to organelles such as melanosomes, platelet dense granules and natural killer cell lytic granules (Marks *et al*. 2013). In trypanosomatids, the LRO classification have been attributed to acidocalcisomes (Docampo *et al*. 2010), acidic organelles rich in polyphosphate complexed with cations, mainly calcium.

Trypomastigotes' protease-containing compartments were first designated LROs (Sant'Anna *et al*. 2008*a*). However, the present demonstration that they may contain endocytic cargo together with the acid hydrolases shown in 2008 turns their classification as LROs inadequate. Moreover, no other organelles were characterized as lysosomes in *T. cruzi* yet. Vesicles containing aryl sulphatase were cytochemically detected in epimastigotes (Adade *et al*. 2007), but no further characterization were performed. Classic lysosomal enzyme markers, as acid phosphatase, although localized by cytochemistry in cytoplasmic organelles of many trypanosomatids, were not found in endocytic vesicles or reservosomes in *T. cruzi*. Instead of this, acid phosphatase was localized in plasma membrane (Nagakura *et al*. 1985; Soares and De Souza, 1988). Other mammalian lysosomal markers, as LAMP 1, LAMP 2 and lgp 120 (Lewis *et al*. 1985) were also not found by immunocytochemistry (Soares *et al*. 1992). The absence of specific markers for epimastigote reservosomes and trypomastigote protease-containing compartments in *T. cruzi* may be a lacking puzzle piece to ensure that they are true lysosomes.

Considering all data concerning epimastigote reservosomes ultrastructure and composition and few data concerning the function of the correspondent organelles in metacyclic trypomastigotes, at present their classification as lysosome-like compartments looks more adequate. The evaluation of internal pH of individual reservosomes and lysosome-like compartments of *T. cruzi* will probably reveal a range of compartments of different maturation grades.

SUPPLEMENTARY MATERIAL

The supplementary material for this article can be found at https://doi.org/10.1017/S0031182016002602

ACKNOWLEDGEMENTS

We are grateful for the technical assistance of Luis Sergio Júnior. We are also grateful to Dr Celso Sant'Anna for critical reading of the manuscript and Lissa C. R. B. Moreira for help with flow cytometry data.

FINANCIAL SUPPORT

This work was supported by Conselho Nacional de Desenvolvimento Científico e Tecnológico (CNPq), Coordenação de Aperfeiçoamento de Pessoal de Nível Superior (CAPES), Financiadora de Estudos e Projetos (FINEP), Programas Núcleo de Excelência (PRONEX) and Cientista do Nosso Estado da Fundação Carlos Chagas Filho de Amparo à Pesquisa no Estado do Rio de Janeiro (FAPERJ).

CONFLICT OF INTEREST

None.

REFERENCES

Adade, C. M., de Castro, S. L. and Soares, M. J. (2007). Ultrastructural localization of *Trypanosoma cruzi* lysosomes by aryl sulphatase cytochemistry. *Micron* **38**, 252–256.

Bayer-Santos, E., Aguilar-Bonavides, C., Rodrigues, S. P., Cordero, E. M., Marques, A. F., Varela-Ramirez, A., Choi, H., Yoshida, N., da Silveira, J. F. and Almeida, I. C. (2013). Proteomic analysis of *Trypanosoma cruzi* secretome: characterization of two populations of extracellular vesicles and soluble proteins. *Journal of Proteome Research* **12**, 883–897.

Camargo, E. P. (1964). Growth and differentiation in *Trypanosoma cruzi*. I. Origin of metacyclic trypanosomes in liquid media. *Revista do Instituto de Medicina Tropical de Sao Paulo* **6**, 93–100.

Cardoso, J., Soares, M. J., Menna-Barreto, R. F., Le Bloas, R., Sotomaior, V., Goldenberg, S. and Krieger, M. A. (2008). Inhibition of proteasome activity blocks *Trypanosoma cruzi* growth and metacyclogenesis. *Parasitology Research* **103**, 941–951.

Contreras, V. T., Salles, J. M., Thomas, N., Morel, C. M. and Goldenberg, S. (1985). *In vitro* differentiation of *Trypanosoma cruzi* under chemically defined conditions. *Molecular & Biochemical Parasitology* **16**, 315–327.

De Souza, W. (2002). Basic cell biology of *Trypanosoma cruzi*. *Current Pharmaceutical Design* **8**, 269–285.

de Souza, W., Sant'Anna, C. and Cunha-e-Silva, N. L. (2009). Electron microscopy and cytochemistry analysis of the endocytic pathway of pathogenic protozoa. *Progress in Histochemistry and Cytochemistry* **44**, 67–124.

Docampo, R., Ulrich, P. and Moreno, S. N. (2010). Evolution of acidocalcisomes and their role in polyphosphate storage and osmoregulation in eukaryotic microbes. *Philosophical Transactions of the Royal Society of London B, Biological Sciences* **365**, 775–784.

Drobne, D., Milani, M., Leser, V., Tatti, F., Zrimec, A., Znidarsic, N., Kostanjsek, R. and Strus, J. (2008). Imaging of intracellular spherical lamellar structures and tissue gross morphology by a focused ion beam/scanning electron microscope (FIB/SEM). *Ultramicroscopy* **108**, 663–670.

Figueiredo, R. C., Rosa, D. S. and Soares, M. J. (2000). Differentiation of *Trypanosoma cruzi* epimastigotes: metacyclogenesis and adhesion to substrate are triggered by nutritional stress. *Journal of Parasitology* **86**, 1213–1218.

Franke de Cazzulo, B. M., Martinez, J., North, M. J., Coombs, G. H. and Cazzulo, J. J. (1994). Effects of proteinase inhibitors on the growth and differentiation of *Trypanosoma cruzi*. *FEMS Microbiology Letters* **124**, 81–86.

Garcia-Silva, M. R., das Neves, R. F., Cabrera-Cabrera, F., Sanguinetti, J., Medeiros, L. C., Robello, C., Naya, H., Fernandez-Calero, T., Souto-Padron, T., de Souza, W. and Cayota, A. (2014). Extracellular vesicles shed by *Trypanosoma cruzi* are linked to small RNA pathways, life cycle regulation, and susceptibility to infection of mammalian cells. *Parasitology Research* **113**, 285–304.

Kessler, R. L., Gradia, D. F., Pontello Rampazzo Rde, C., Lourenco, E. E., Fidencio, N. J., Manhaes, L., Probst, C. M., Avila, A. R. and Fragoso, S. P. (2013). Stage-regulated GFP Expression in *Trypanosoma cruzi*: applications from host–parasite interactions to drug screening. *PLoS ONE* **8**, e67441.

Lewis, V., Green, S. A., Marsh, M., Vihko, P., Helenius, A. and Mellman, I. (1985). Glycoproteins of the lysosomal membrane. *Journal of Cell Biology* **100**, 1839–1847.

Marks, M. S., Heijnen, H. F. and Raposo, G. (2013). Lysosome-related organelles: unusual compartments become mainstream. *Current Opinion in Cell Biology* **25**, 495–505.

Nagakura, K., Tachibana, H. and Kaneda, Y. (1985). Alteration of the cell surface acid phosphatase concomitant with the morphological transformation in *Trypanosoma cruzi*. *Comparative Biochemistry and Physiology B* **81**, 815–817.

Reynolds, E. S. (1963). Use of lead citrate at high Ph as an electron-opaque stain in electron microscopy. *Journal of Cell Biology* **17**, 208.

Roth, J. (1983). Application of lectin–gold complexes for electron microscopic localization of glycoconjugates on thin sections. *Journal of Histochemistry and Cytochemistry* **31**, 987–999.

Sant'Anna, C., Parussini, F., Lourenco, D., de Souza, W., Cazzulo, J. J. and Cunha-e-Silva, N. L. (2008*a*). All *Trypanosoma cruzi* developmental forms present lysosome-related organelles. *Histochemistry and Cell Biology* **130**, 1187–1198.

Sant'Anna, C., Pereira, M. G., Lemgruber, L., de Souza, W. and Cunha e Silva, N. L. (2008*b*). New insights into the morphology of *Trypanosoma cruzi* reservosome. *Microscopy Research and Technique* **71**, 599–605.

Sant'Anna, C., Nakayasu, E. S., Pereira, M. G., Lourenco, D., de Souza, W., Almeida, I. C. and Cunha, E. S. N. L. (2009). Subcellular proteomics of *Trypanosoma cruzi* reservosomes. *Proteomics* **9**, 1782–1794.

Slot, J. W. and Geuze, H. J. (1985). A new method of preparing gold probes for multiple-labeling cytochemistry. *European Journal of Cell Biology* **38**, 87–93.

Soares, M. J. and De Souza, W. (1988). Cytoplasmic organelles of trypanosomatids: a cytochemical and stereological study. *Journal of Submicroscopic Cytology and Pathology* **20**, 349–361.

Soares, M. J. and de Souza, W. (1991). Endocytosis of gold-labeled proteins and LDL by *Trypanosoma cruzi*. *Parasitology Research* **77**, 461–468.

Soares, M. J., Souto-Padron, T., Bonaldo, M. C., Goldenberg, S. and de Souza, W. (1989). A stereological study of the differentiation process in *Trypanosoma cruzi*. *Parasitology Research* **75**, 522–527.

Soares, M. J., Souto-Padron, T. and De Souza, W. (1992). Identification of a large pre-lysosomal compartment in the pathogenic protozoon *Trypanosoma cruzi*. *Journal of Cell Science* **102**, 157–167.

Trocoli Torrecilhas, A. C., Tonelli, R. R., Pavanelli, W. R., da Silva, J. S., Schumacher, R. I., de Souza, W., NC, E. S., de Almeida Abrahamsohn, I., Colli, W. and Manso Alves, M. J. (2009). *Trypanosoma cruzi*: parasite shed vesicles increase heart parasitism and generate an intense inflammatory response. *Microbes and Infection* **11**, 29–39.

Vidal, J. C., Alcantara, C. L., de Souza, W. and Cunha, E. S. N. L. (2016). Loss of the cytostome–cytopharynx and endocytic ability are late events in *Trypanosoma cruzi* metacyclogenesis. *Journal of Structural Biology* **196**, 319–328.

Vieira, M., Rohloff, P., Luo, S., Cunha-e-Silva, N. L., de Souza, W. and Docampo, R. (2005). Role for a P-type H+-ATPase in the acidification of the endocytic pathway of *Trypanosoma cruzi*. *Biochemical Journal* **392**, 467–474.